Modulated structure of $Ba_6ZnIr_4O_{15}$; a comparison with $Ba_6CuIr_4O_{15}$ and $SrMn_{1-x}Co_xO_{3-y}$

Peter D. Battle,[a] Graeme R. Blake,[a] Jacques Darriet,[b] Jonathan G. Gore[a] and François Weill[b]

[a]*Inorganic Chemistry Laboratory, South Parks Road, Oxford, UK OX1 3QR*

[b]*ICMCB, Chateau Brivazac, Av. Dr. Schweitzer, 33608 Pessac Cedex, France*

The new phase $Ba_6CuIr_4O_{15}$ has been shown by powder X-ray diffraction to be a member of the perovskite-related structural family $A_{3n+3}A'_nB_{n+3}O_{6n+9}$ with $n=1$; space group $R32$, $a=10.1196(3)$, $c=13.4097(4)$ A. The trigonal-prismatic A′ sites and the octahedral B sites are both occupied by a disordered distribution of Ir and Cu. A combination of electron microscopy and X-ray diffraction has shown that $Ba_6ZnIr_4O_{15}$ has a related incommensurate structure with $a\approx10.1$, $c\approx4.4$ A and a modulation vector $\boldsymbol{q}=\boldsymbol{a}^*+0.35\boldsymbol{c}^*$. Alternatively, $Ba_6ZnIr_4O_{15}$ can be considered as a composite of trigonal (cell 1) and rhombohedral (cell 2) substructures with $a_1=a_2=10.1228(9)$ $c_1=4.4099(6)$, $c_2=2.6982(2)$ A. It is shown that the same structural formalism can be used to describe the incommensurate hexagonal phase of $SrMn_{1-x}Co_xO_{3-y}$.

There has been a recent upsurge of interest in the solid-state chemistry of ternary and quaternary oxides of the platinum metals. This has been driven largely by the observation that many of these compounds adopt crystal structures which apparently contain one-dimensional chains of transition-metal coordination polyhedra, thus introducing the possibility of unusual electronic properties, but it has also been driven in part by recent progress in structural chemistry, in particular the recognition that these structures are related to that of perovskite.[1] The 2H hexagonal perovskite structure[2] is often thought of as a pseudo-hcp stack of AO_3 layers (A is usually an alkaline-earth element) with transition-metal cations, B, occupying octahedral holes between the layers to give the stoichiometry ABO_3. This is sometimes conveniently referred to in terms of A_3O_9 layers, leading to the stoichiometry $A_3B_3O_9$. It has now been recognized that the structures of many oxides, the stoichiometry of which is not obviously related to that of perovskite, can be considered within the same structural framework if we allow for the inclusion of modified layer types within the stacking sequence. For example, an ordered removal of three oxide ions from an A_3O_9 layer leads to the formation of an A_3O_6 layer, and the stacking sequence $(A_3O_6)_3(A_3O_9)$ leads to the overall stoichiometry A_4O_9. It has recently been shown[3] that this stacking sequence occurs in the crystal structure of $Sr_4Ru_2O_9$ (Fig. 1), with the Ru^V cations occupying the octahedral sites which are formed between the layers. In addition to these octahedral sites, the hexagonal stacking of A_3O_6 layers leads to the creation of cation sites (A′) with trigonal-prismatic coordination by oxygen. The creation of these sites, which lie within the A_3O_6 layers, is made possible by the reduced oxide concentration therein (Fig. 2). The trigonal-prismatic sites are unoccupied in $Sr_4Ru_2O_9$. In compounds in which they are occupied, the stoichiometry of the layers is properly described as $A_3A'O_6$, where A and A′ may be the same element. The well known Sr_4PtO_6[4] structure (Fig. 3) can then be described as consisting of the stacking sequence $(A_3A'O_6)_\infty$, with A = A′ = Sr and with Pt occupying the octahedral (B) sites between the layers. Many ternary oxides of Pt and Ir crystallize with this structure, for example Ca_4IrO_6,[5] Ca_4PtO_6,[6] Sr_4IrO_6[7] and Ba_4PtO_6.[8] More recently, several quaternary members of this series with $A\neq A'$ have been reported, including Ca_3CuIrO_6,[9] $Ca_{3.5}Cu_{0.5}PtO_6$,[10] Sr_3MIrO_6 (M = Li, Na, Ca, Ni, Cu, Zn, Cd),[11–14] Sr_3MPtO_6 (M = Ni, Cu, Zn),[15–17] $Sr_3CuPt_{0.5}Ir_{0.5}O_6$,[18] Sr_3NiYbO_6[19] and Ba_3NaIrO_6;[20] the recent preparation of $Ca_3Co_2O_6$[21] provides an interesting example of a compound in which A′ = B.

Other stoichiometries can be envisaged if the stacking sequence of $(A_3A'O_6)$ and (A_3O_9) layers is allowed to vary, and the general case may be written as $(A_3A'O_6)_n(A_3O_9)$, that is an (A_3O_9) layer is inserted after every $n(A_3A'O_6)$ layers; filling the octahedral and trigonal-prismatic holes then leads to the composition $A_{3n+3}A'_nB_{n+3}O_{6n+9}$. The first example of an $n=2$ phase was reported recently by Campa *et al.*[22] and a number of $n=1$ phases (Fig. 4) have been described previously, for example $Ba_6Ni_5O_{15}$[23] and $Sr_6Co_5O_{15}$;[24] these phases also have A′ = B. We now report the synthesis of two further $n=1$ phases, $Ba_6MIr_4O_{15}$, (M = Cu and Zn) in which $A'\neq A\neq B$, the strategy being to introduce a metal from the third transition series into the chains of polyhedra parallel to the z axis, in the hope that the introduction of a 5d cation might enhance the electrical conductivity of the system. Our work has revealed unexpected differences in the crystal chemistry of these two compounds, and in this paper we contrast the relatively simple structure of $Ba_6CuIr_4O_{15}$ with the modulated structure that we have encountered in the case of $Ba_6ZnIr_4O_{15}$. Furthermore, we show that the structural chemistry of the system $SrMn_{1-x}Co_xO_{3-y}$, previously described as an incommensurate hexagonal perovskite,[25] can be accounted for within the formalism developed to describe $Ba_6ZnIr_4O_{15}$.

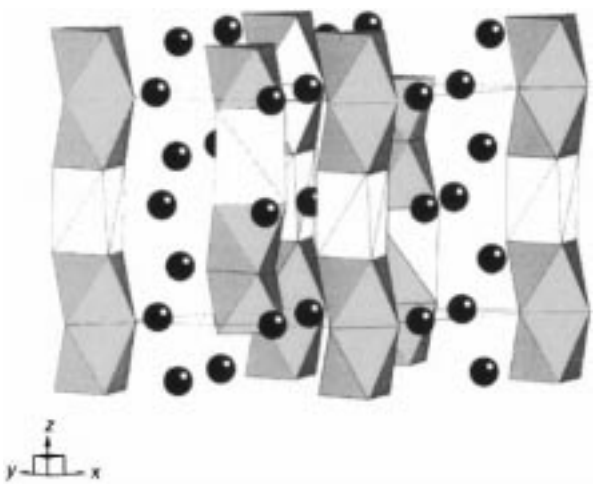

Fig. 1 Crystal structure of $Sr_4Ru_2O_9$. RuO_6 octahedra are shaded, empty trigonal-prismatic sites are unshaded. Shaded circles represent Sr.

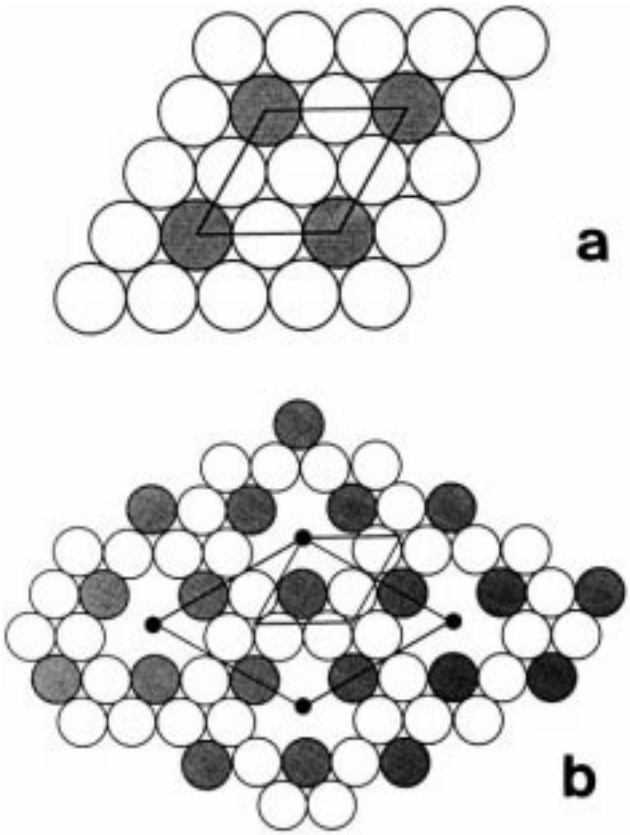

Fig. 2 Layers of different stoichiometry in $A_{3n+3}A'_nB_{n+3}O_{6n+9}$; a, an A_3O_9 layer; A represented by shaded circles, O by empty circles; b, an A_3O_6 layer with trigonal-prismatic sites marked by solid circles; the two-dimensional unit cells of both layer types are shown, with $a' = \sqrt{3}a$.

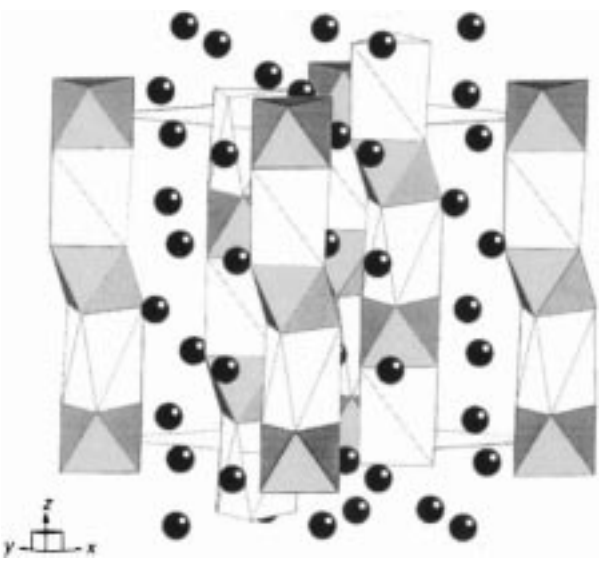

Fig. 3 Crystal structure of Sr_4PtO_6. PtO_6 octahedra are shaded, SrO_6 trigonal prisms are unshaded. Shaded circles also represent Sr.

Experimental

Ba_6CuIrO_{15} was synthesized by heating a well ground, stoichiometric mixture of $BaCO_3$, CuO and Ir metal in an alumina crucible. The mixture was initially fired at 650 °C, then the temperature was raised to 1050 °C, and subsequently to 1100 °C for 2 days; the reactions were all carried out in air. The Cu content of the final product was determined using AAS; the presence of two transition-metal species prevented a reliable determination of the oxygen content by iodometric titration in this case. $Ba_6ZnIr_4O_{15}$ was prepared by prefiring appropriate

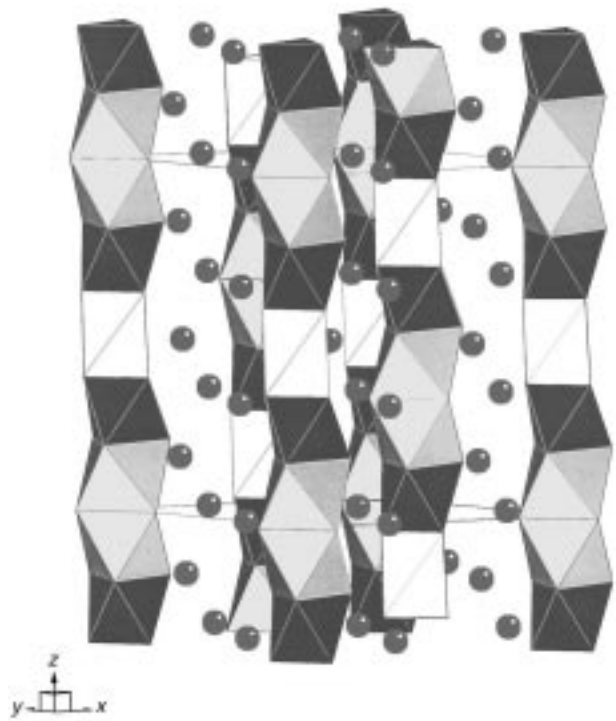

Fig. 4 Crystal structure of $Sr_6Co_5O_{15}$. Shaded octahedral and unshaded trigonal-prismatic sites are occupied by Co. Shaded circles represent Sr.

quantities of $BaCO_3$, ZnO and Ir metal at 650 °C, followed by further heating at 900 °C (12 h) and 1200 °C (40 h). The chemical composition of the product was determined by AAS and iodometric titration. A Siemens D5000 diffractometer, operating with Cu-Kα_1 radiation in Bragg–Brentano geometry, was used to record the X-ray powder diffraction pattern of both products. Data were collected in the angular range $5 \leqslant 2\theta/^\circ \leqslant 100$ with a 2θ step size of 0.02°. Selected area electron diffraction (SAED) patterns were recorded with a JEOL 2000FX microscope, operating at 200 kV. The specimens were crushed in alcohol and a drop of the suspension was deposited on a holey carbon supported grid.

Results

AAS showed that the Cu content of our reaction product (3.3%) was in excellent agreement with that expected for the formula Ba_6CuIrO_{15} (3.3%). The X-ray diffraction pattern collected on this sample could be indexed in space group $R32$, with unit-cell parameters $a = 10.1196(3)$, $c = 13.4097(4)$ A. The

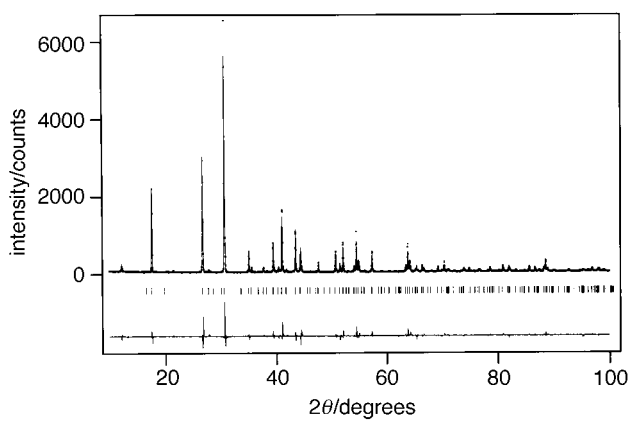

Fig. 5 Observed, calculated and difference X-ray powder diffraction profiles for $Ba_6CuIr_4O_{15}$. Reflection positions are marked.

Table 1 Structural parameters for $Ba_6CuIr_4O_{15}$[a]

atom	site	occupancy	x	y	z
Ba(1)	9d	1.0	0.325(1)	0	0
Ba(2)	9e	1.0	0.657(1)	0	
Ir(1)	6c	0.884(6)	0	0	0.0981(8)
Ir(2)	6c	0.797(6)	0	0	0.2828(6)
Ir(3)	3b	0.64(2)	0	0	0.5
Cu(1)	6c	0.116(6)	0	0	0.0981(8)
Cu(2)	6c	0.203(6)	0	0	0.2828(6)
Cu(3)	3b	0.36(2)	0	0	0.5
O(1)	18f	1.0	0.479(9)	0.163(9)	0.526(5)
O(2)	9d	1.0	0.18(1)	0.18(1)	0
O(3)	18f	1.0	0.34(1)	0.526(7)	0.044(4)

[a] $a = 10.1196(3)$, $c = 13.4097(4)$ Å; overall isotropic temperature factor $B = 1.01(7)$ Å^2.

electron diffraction pattern did not contain any features which were inconsistent with this choice of space group and unit cell. The crystal structure was refined by profile analysis of the X-ray data, using the GSAS program package.[26,27] The $n=1$ structure of $Ba_6Ni_5O_{15}$[23] was used as a starting model. This structure has Ni cations distributed over three crystallographic sites, two of which (M1 and M2) lie within face-sharing oxygen octahedra (Fig. 4), whilst the other (M3) has trigonal-prismatic coordination. It became apparent during our preliminary refinements that the Cu and Ir cations are disordered over these three sites, and their occupancies were therefore included in the refinement, along with eleven variable atomic coordinates and an overall isotropic temperature factor. The overall profile parameters included in the analysis were the scale factor, two unit-cell parameters, a counter zeropoint correction, eight coefficients of a Chebyshev polynomial background function, and five variables to describe the width of the pseudo-Voigt Bragg peaks. This parameter set resulted in a weighted profile R-factor $R_{wpr} = 16.0\%$, and an intensity R-factor $R_I = 10.6\%$. The observed and calculated diffraction profiles, along with their difference, are plotted in Fig. 5. The refined structural parameters are listed in Table 1, and the derived bond lengths and bond angles are listed in Table 2.

AAS found a Zn content of 3.6% in our sample of $Ba_6ZnIr_4O_{15}$, in reasonable agreement with the expected value (3.4%). Iodometric titrations led to a value of 4.00(2) for the oxidation state of Ir, in excellent agreement with the nominal value. However, the analysis of the X-ray diffraction data did not progress smoothly in this case. Certain peaks in the diffraction pattern could be indexed as $\{hk0\}$ reflections with $a = b \approx 10.1$ Å, but we were unable to find a set of unit cell parameters which enabled us to account for those peaks having $l \neq 0$. Close inspection of the electron diffraction patterns revealed a complex distribution of intensity which could not

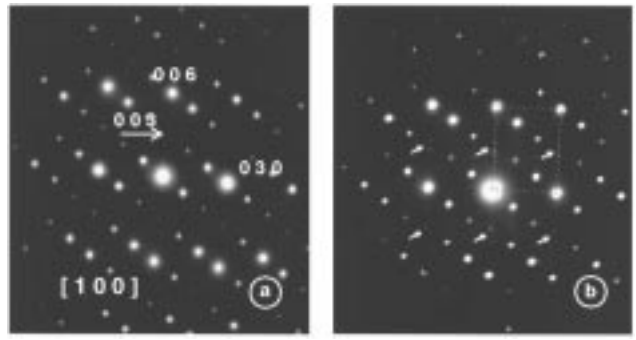

Fig. 6 Electron diffraction pattern of (a) $Ba_6Ir_4CuO_{15}$ and (b) $Ba_6Ir_4ZnO_{15}$. The rectangle indicates the net of the main reflections and the arrows point out the double spots due to the incommensurate modulation.

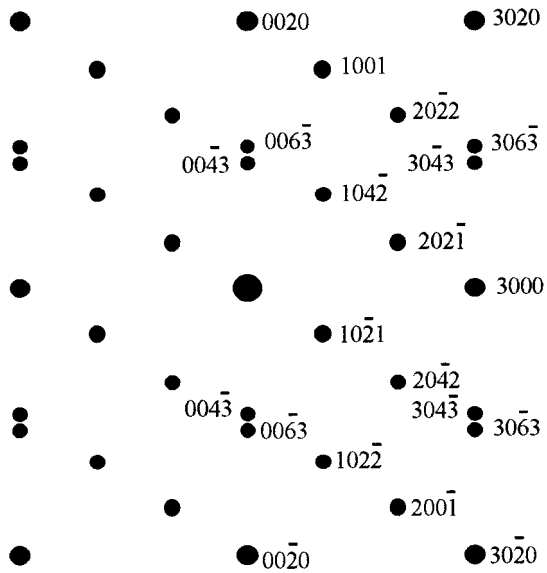

Fig. 7 Schematic representation of a section of Fig. 6(b). The four-dimensional indexing relates to the unit cell having parameters: $a \approx 10.1$ Å, $c_1 \approx 4.4$ Å and $c_2 \approx 2.7$ Å.

Table 2 Bond lengths (Å) and bond angles (degrees) for $Ba_6CuIr_4O_{15}$

Ba(1)−O(1)	2 × 2.98(5), 2 × 2.49(8)	Ir(1)/Cu(1)−Ir(1)/Cu(1)	1 × 2.63(2)
Ba(1)−O(2)	2 × 2.85(1)	Ir(1)/Cu(1)−Ir(2)/Cu(2)	2 × 2.48(2)
Ba(1)−O(3)	2 × 3.02(9), 2 × 3.04(9)	Ir(2)/Cu(2)−Ir(3)/Cu(3)	2 × 2.912(8)
Ba(2)−O(1)	2 × 2.81(7), 2 × 3.00(7)		
Ba(2)−O(2)	2 × 2.70(7)	Ir(1)/Cu(1)−O(1)	3 × 2.21(9)
Ba(2)−O(3)	2 × 2.62(5), 2 × 3.40(4)	Ir(1)/Cu(1)−O(2)	3 × 2.24(10)
O(1)−O(1)	2 × 3.2(2), 2.9(2)		
O(1)−O(2)	2 × 3.08(7)	Ir(2)/Cu(2)−O(1)	3 × 2.19(7)
O(1)−O(3)	3.06(9), 2.91(9)	Ir(2)/Cu(2)−O(3)	3 × 1.91(5)
O(2)−O(2)	3.2(2)		
O(2)−O(3)	2 × 3.1(1)	Ir(3)/Cu(3)−O(3)	6 × 2.18(4)
O(3)−O(3)	2 × 2.48(8)		
O(1)−Ir(1)/Cu(1)−O(1)	3 × 91(2)	O(1)−Ir(2)/Cu(2)−O(1)	3 × 92(3)
O(1)−Ir(1)/Cu(1)−O(2)	3 × 93(2)	O(1)−Ir(2)/Cu(2)−O(3)	3 × 96(2)
O(1)−Ir(1)/Cu(1)−O(2)	3 × 88(2)	O(1)−Ir(2)/Cu(2)−O(3)	3 × 90(3)
O(1)−Ir(1)/Cu(1)−O(2)	3 × 176(2)	O(1)−Ir(2)/Cu(2)−O(3)	3 × 171(2)
O(2)−Ir(1)/Cu(1)−O(2)	3 × 89(3)	O(3)−Ir(2)/Cu(2)−O(3)	3 × 81(2)
	O(3)−Ir(3)/Cu(3)−O(3)	6 × 69(2)	
	O(3)−Ir(3)/Cu(3)−O(3)	3 × 143(5)	
	O(3)−Ir(3)/Cu(3)−O(3)	3 × 140(4)	
	O(3)−Ir(3)/Cu(3)−O(3)	3 × 98(3)	

Table 3 X-Ray powder diffraction data for $Ba_6ZnIr_4O_{15}$[a]

h	k	l	m	d_{obs}	I_{obs}	d_{calc}	h	k	l	m	d_{obs}	I_{obs}	d_{calc}
1	0	−2	1	7.0880	2.9	7.0849	0	5	0	1	1.4700	2.9	1.4702
1	1	0	0	5.0611	29.3	5.0614	6	0	0	0	1.4611	13.1	1.4611
1	1	1	0	3.3244	38.6	3.3249	4	1	2	0	1.4448	4.5	1.4450
2	1	−2	1	3.1945	1.5	3.1951	2	4	0	1	1.4118	3.8	1.4118
3	0	0	0	2.9211	100	2.9222	5	2	0	0	1.4037	2.5	1.4038
1	0	0	1	2.5792	7.2	2.5788	5	1	0	1	1.3600	3.1	1.3599
2	2	0	0	2.5310	2.9	2.5307	5	2	1	0	1.3377	5.2	1.3376
1	3	−2	1	2.3832	1.9	2.3835	2	0	0	2	1.2894	1.5	1.2894
0	2	0	1	2.2979	10.9	2.2978	4	3	0	1	1.2710	2.4	1.2712
2	2	1	0	2.1949	25.7	2.1950	1	2	0	2	1.2495	1.5	1.2495
4	0	−2	1	2.1554	1.4	2.1563	4	4	1	0	1.2164	3.3	1.2163
2	1	0	1	2.0919	15.3	2.0923	5	2	2	0	1.1839	2.4	1.1842
1	1	2	0	2.0206	5.8	2.0215	4	1	3	0	1.1657	1.8	1.1656
4	1	0	0	1.9130	5.2	1.9130	7	1	0	0	1.1611	1.6	1.1612
1	3	0	1	1.8063	7.8	1.8062	3	5	0	1	1.1359	2.9	1.1360
4	1	1	0	1.7552	13.0	1.7550	7	0	0	1	1.1359	2.9	1.1360
4	0	0	1	1.7014	3.4	1.7012	7	1	1	0	1.1229	2.6	1.1229
3	3	0	0	1.6871	17.6	1.6871	6	2	0	1	1.1084	2.4	1.1084
2	2	2	0	1.6622	4.2	1.6625	6	3	0	0	1.1044	6.0	1.1045
3	2	0	1	1.6125	8.2	1.6125							

[a] $a = 10.1228(9)$, $c_1 = 4.4099(6)$, $c_2 = 2.6982(2)$ Å; All observed maxima with $I_{obs} > 1.3\%$ are accounted for.

be accounted for using a conventional three-dimensional unit cell. This is illustrated by a comparison of the two patterns shown in Fig. 6(a) and 6(b), which were collected on $Ba_6CuIr_4O_{15}$ and $Ba_6ZnIr_4O_{15}$ respectively; both patterns show the [100] zone. The most obvious difference is that the reflection indexed as (003) in Fig. 6(a) appears to be split into two in Fig. 6(b). Closer inspection reveals that the only reflections which are located at the same place in both patterns are those at the corners of the rectangular net based on the reflections indexed as (030) and (006) in Fig. 6(a). Consequently, in order to account for the pattern in Fig. 6(b), it is necessary to introduce an incommensurate modulation around each reflection on the rectangular net. If this approach is adopted, the six spots which surround each one on the net are indexed as satellites; the intensity of the satellites decreases as their order increases. The diffraction pattern of $Ba_6ZnIr_4O_{15}$ can then be described using a trigonal unit cell having direct parameters $a \approx 10.1$ Å, $c \approx 4.4$ Å and the modulation vector $\boldsymbol{q}^* = \boldsymbol{a}^* + 0.35\boldsymbol{c}^*$. Alternatively,[28] the pattern shown in Fig. 6(b) can be indexed, as is illustrated in Fig. 7, using a four-dimensional trigonal cell with $a \approx 10.1$, $c_1 \approx 4.4$ and $c_2 \approx 2.7$ Å. Such a description has been used previously[29,30] to account for the structure of $[Ba_x][(Pt,Cu)O_3]$. By analogy with that work, our observations can be explained if our sample of $Ba_6ZnIr_4O_{15}$ is considered to be a composite crystal, comprising two subsystems. The first of these consists of the Ba cations, which are located in the channels formed by the second subsystem, that is the Zn/Ir—O polyhedra which form chains parallel to the z axis. Having used electron diffraction to establish the complex nature of the structure we were able to index the X-ray diffraction pattern using four indices (h,k,l,m) and three unit-cell parameters; $a = 10.1221$, $c_1 = 4.4073$, $c_2 = 2.6982$ Å. The full, indexed list of observed Bragg reflections is presented in Table 3. The space groups of the two subsystems cannot be assigned unambiguously from our data, although that of cell 1 appears to be trigonal ($P3c1$ or $P\bar{3}c1$) and cell 2 is rhombohedral with no glide plane present.

Discussion

The refinement of the crystal structure of $Ba_6CuIr_4O_{15}$ is not of the highest precision, nor can it be expected to be given that we are using X-ray powder diffraction to analyse a compound that contains a variety of light and heavy atoms distributed over eight crystallographic sites. The difficulties are compounded by the presence of a disordered distribution of two transition-metal species over three sites. Nevertheless, the data undoubtedly suffice to establish the basic structural features of this compound. The bond lengths listed in Table 2 are all chemically reasonable, with the possible exception of an O(3)—O(3) distance of 2.48(8) Å. However, the standard deviation on this distance is large enough to bring it into the range of acceptable values. The metal–metal distances within the tetramer of face-sharing octahedra are very short [2.63(2) and 2.48(2) Å], as were those observed previously in $Ba_6Ni_5O_{15}$[23] and $Sr_6Co_5O_{15}$;[24] the distance between transition-metal cations on octahedral and trigonal-prismatic sites is somewhat longer [2.912(8) Å]. It is interesting to compare the structure of $Ba_6Ir_4CuO_{15}$ with that of Sr_3CuIrO_6, an $n = \infty$ compound in which the octahedral sites are occupied only by Ir, and the Cu atoms are displaced from the centre of the trigonal-prismatic site into one of the rectangular faces of the polyhedron, thus creating chains in which IrO_6 octahedra share edges with CuO_4 squares.[14] The symmetry is consequently reduced to monoclinic ($C2/c$). If the Ir and Cu atoms in $Ba_6CuIr_4O_{15}$ were ordered with the Cu atoms occupying the trigonal-prismatic sites, a similar distortion to a monoclinic cell would be possible. However, trial refinements established that this symmetry lowering does not occur, and we believe that the cation disorder quenches the cooperative Jahn–Teller distortion which the degenerate electronic ground state of Cu^{2+} might otherwise induce. The crystal structure of $Ba_6CuIr_4O_{15}$, although disordered, is commensurate when the sample is prepared in the manner described above. It therefore serves to provide a contrast with the complex crystal chemistry of $Ba_6ZnIr_4O_{15}$. We have not analysed the intensity distribution in the diffraction pattern of this incommensurate phase, merely the peak distribution, and we are therefore unable to comment with any confidence on the detailed structural chemistry within the two substructures which constitute the composite structure. However, the very occurrence of this incommensurate phase raises a number of questions. It is important to establish if the

Table 4 Unit-cell parameters for $SrMn_{1-x}Co_xO_{3-y}$

x	a	c_1	c_2
0.40	9.576(4)	4.032(2)	2.548(2)
0.42	9.572(3)	4.032(2)	2.548(1)
0.45	9.572(5)	4.009(2)	2.553(2)
0.50	9.571(5)	3.974(2)	2.558(3)
0.55	9.560(5)	3.946(3)	2.561(3)

Table 5 X-Ray powder diffraction data for $SrMn_{1-x}Co_xO_{3-y}$

				$x=0.40$		$x=0.42$		$x=0.45$		$x=0.50$		$x=0.55$	
h	k	l	m	d_{obs}	d_{calc}	d_{obs}	d_{calc}	d_{obs}	d_{calc}	d_{obs}	d_{calc}	d_{obs}	d_{calc}
1	0	−2	1	6.282	6.283	6.281	6.290	6.204	6.196	(6.05)	6.069	(6.03)	5.965
1	1	0	0	4.778	4.786	4.768	4.786	4.794	4.786	4.797	4.786	4.795	4.780
0	2	−2	1	3.807	3.807	3.803	3.809	3.791	3.788	3.758	3.758	(3.74)	3.730
1	1	1	0	3.084	3.083	3.082	3.084	3.078	3.073	3.061	3.057	3.046	3.043
3	0	0	0	2.762	2.763	2.760	2.763	2.767	2.763	2.767	2.763	2.763	2.760
1	0	0	1	2.436	2.436	2.434	2.435	2.437	2.440	2.440	2.444	—	—
2	2	0	0	2.395	2.393	2.392	2.393	2.394	2.393	2.396	2.393	2.393	2.390
1	3	−2	1	2.238	2.236	2.234	2.237	2.235	2.232	2.228	2.226	2.224	2.219
1	3	−1	1	2.181	2.182	2.179	2.182	2.185	2.185	2.190	2.189	2.191	2.190
0	2	0	1	2.168	2.171	2.168	2.171	2.172	2.174	2.180	2.177	2.183	2.178
2	2	1	0	2.058	2.058	2.057	2.058	2.055	2.055	2.051	2.050	2.045	2.044
0	0	2	0	2.017	2.016	2.014	2.016	2.007	2.004	1.991	1.987	1.975	1.973
2	1	0	1	1.976	1.977	1.974	1.977	1.980	1.979	1.983	1.981	—	—
3	2	−2	1	—	—	1.864	1.866	1.864	1.863	1.860	1.860	1.857	1.855
1	1	2	0	1.857	1.858	1.856	1.858	1.851	1.849	1.836	1.835	1.826	1.824
1	3	0	1	1.706	1.707	1.706	1.707	1.708	1.709	1.711	1.710	1.710	1.710
4	1	1	0	1.650	1.650	1.649	1.650	1.650	1.649	1.648	1.646	1.645	1.643
3	0	2	0	1.628	1.628	1.628	1.629	1.623	1.623	1.614	1.613	1.606	1.605
3	3	0	0	1.595	1.595	1.594	1.595	1.595	1.595	1.596	1.595	1.594	1.593
2	2	2	0	1.542	1.542	1.541	1.542	1.537	1.537	1.530	1.529	1.522	1.522
3	2	0	1	1.524	1.524	1.523	1.524	1.526	1.525	1.527	1.526	1.527	1.526
5	1	−1	1	1.456	1.456	1.454	1.456	1.458	1.457	1.458	1.458	1.459	1.457
0	5	0	1	1.390	1.390	1.389	1.390	1.391	1.391	1.392	1.391	1.391	1.390
6	0	0	0	1.382	1.382	1.381	1.382	1.382	1.382	1.382	1.382	1.381	1.380

coexistence of trigonal-prismatic and octahedral sites along the z axis is in some way responsible for the effect, and how common this behaviour is in $A_{3n+3}A'_nB_{n+3}O_{6n+9}$ compounds. It will also be interesting to see if the modulation vector can be controlled by modification of the synthesis conditions, and whether concomitant control of the electronic properties can be established. Experiments designed to answer these questions are now in progress. It is also interesting to review the structural chemistry of perovskite related oxides in order to identify incompletely characterised compounds which may show similar structural features. $SrMn_{1-x}Co_xO_{3-y}$ has previously been described[25] as an incommesurate hexagonal (icH) perovskite but the details of the structure are still uncertain. EXAFS data showed the presence of two Co—Co/Mn distances (2.56 and 2.87 A), but only one Mn—Co/Mn distance (2.53 A), from which it was concluded that the Mn cations are likely to occur only in the face-sharing octahedra characteristic of a hexagonal perovskite, whereas the Co catons occur in face-sharing octahedra (Co—Co ≈ 2.5 A) and also in another coordination environment. The latter was not identified with any confidence, although edge-sharing octahedra were suggested. We have now re-indexed the published X-ray powder diffraction patterns, and the level of agreement shown in Tables 4 and 5 demonstrates that the $SrMn_{1-x}Co_xO_{3-y}$ system can also be regarded as having a composite structure related to that of $Ba_6ZnIr_4O_{15}$ and the commensurate analogue $Ba_6CuIr_4O_{15}$. Inspection of the data in Table 2 then leads to the conclusion that the long Co–Co/Mn distance observed by EXAFS corresponds to the separation of a pair of face-sharing octahedral and trigonal-prismatic sites. It is also interesting to review the Sr–Co-O system. Harrison *et al.*[24] have recently shown that the reaction product which had been described for many years as the low-temperature hexagonal form of $SrCoO_{3-y}$ is actually a mixture of Co_3O_4 and $Sr_6Co_5O_{15}$, the latter being isostructural with $Ba_6CuIr_4O_{15}$. It may well be that the reported[31] y-dependence in the X-ray diffraction patterns of these compounds arises because of the composition dependence of the modulation vector of an incommensurate phase. Interestingly, the long (≈2.8 A) Co—Co distance is not seen[32] in the EXAFS pattern of the fully reduced composition, and the M_{oct}—M_{prism} distance determined by X-ray diffraction is only 2.50 A. However, a longer Co—Co distance of 2.8 A is apparent in the EXAFS of oxygen-rich samples. No conclusions can be drawn about this system until further experiments have been carried out, but there is reason to believe that the type of structural chemistry found in $Ba_6ZnIr_4O_{15}$ may also occur in a number of other oxides.

We are grateful to the EPSRC for financial support.

References

1 J. Darriet and M. A. Subramanian, *J. Mater. Chem.*, 1995, **5**, 543.
2 J. J. Lander, *Acta Crystallogr.*, 1951, **4**, 148.
3 C. Dussarrat, J. Fompeyrine and J. Darriet, *Eur. J. Solid State Chem.*, 1995, **32**, 3.
4 J. R. Randall and L. Katz, *Acta Crystallogr.*, 1959, **12**, 519.
5 R. F. Sarkozy, C. W. Moeller and B. L. Chamberland, *J. Solid State Chem.*, 1974, **9**, 242.
6 I. S. Shaplygin and V. B. Lazarev, *Mater. Res. Bull.*, 1975, **10**, 903.
7 A. V. Powell, P. D. Battle and J. G. Gore, *Acta Crystallogr., Sect. C*, 1993, **49**, 189.
8 A. P. Wilkinson and A. K. Cheetham, *Acta Crystallogr., Sect. C*, 1989, **45**, 1672.
9 A. Tomaszewska and H. Muller-Buschbaum, *Z. Anorg. Allg. Chem.*, 1993, **619**, 534.
10 A. Tomaszewska and H. Muller-Buschbaum, *Z. Anorg. Allg. Chem.*, 1992, **617**, 23.
11 S. Frenzen and H. Muller-Buschbaum, *Z. Naturforsch., B*, 1996, **51**, 225.
12 T. N. Nguyen and H. C. zur-Loye, *J. Solid State Chem.*, 1995, **117**, 300.
13 N. Segal, J. F. Vente, T. S. Bush and P. D. Battle, *J. Mater. Chem.*, 1996, **6**, 395.
14 M. Neubacher and H. Muller-Buschbaum, *Z. Anorg. Allg. Chem.*, 1992, **607**, 124.
15 C. Lampe-Onnerud and H. C. zur-Loye, *Inorg. Chem.*, 1996, **35**, 2155.
16 A. P. Wilkinson, A. K. Cheetham, W. Kunnman and A. Kvick, *Eur. J. Solid State Chem.*, 1991, **28**, 453.
17 T. N. Nguyen, D. M. Giaquinta and H. C. zur-Loye, *Chem. Mater.*, 1994, **6**, 1642.
18 T. N. Nguyen, P. A. Lee and H.-C. zur-Loye, *Science*, 1996, **271**, 489.
19 M. James and J. P. Attfield, *J. Mater. Chem.*, 1994, **4**, 575.
20 S. Frenzen and H. Muller-Buschbaum, *Z. Naturforsch., B*, 1996, **51**, 1204.
21 H. Fjellvag, E. Gulbrandsen, S. Aasland, A. Olsen and B. C. Hauback, *J. Solid State Chem.*, 1996, **124**, 190.

22 J. Campa, E. Gutierrez-Puebla, A. Monge, I. Rasines and C. Ruız-Valero, *J. Solid State Chem*., 1996, **126**, 27.
23 J. A. Campa, E. Gutierrez-Puebla, M. A. Monge, I. Rasines and C. Ruız-Valero, *J. Solid State Chem*., 1994, **108**, 230.
24 W. T. A. Harrison, S. L. Hegwood and A. J. Jacobson, *J. Chem. Soc*., *Chem. Commun*., 1995, 1953.
25 P. D. Battle, T. C. Gibb and R. Strange, *J. Solid State Chem*., 1989, **81**, 217.
26 H. M. Rietveld, *J. Appl. Crystallogr*., 1969, **2**, 65.
27 A. C. Larson and R. B. von-Dreele, General Structure Analysis System (GSAS), Los Alamos National Laboratories, Report LAUR 86–748, 1990.
28 T. Janssen, A. Janner, A. Looijenga-Vos and P. M. de-Wolff, *Incommensurate and commensurate modulated structures*, in *International Tables for Crystallography*, 1995, Kluwer, Dordrecht, vol. C.
29 T. Shishido, K. Ukei and T. Fukuda, *J. Alloys Compd*., 1996, **237**, 89.
30 K. Ukei, A.Yamamoto, Y. Watanabe, T. Shishido and T. Fukuda, *Acta Crystallogr., Sect. B*, 1993, **49**, 67.
31 P. D. Battle, T. C. Gibb and A. T. Steel, *J. Chem. Soc., Dalton Trans*., 1988, 83.
32 P. D. Battle, T. C. Gibb and A. T. Steel, *J. Chem. Soc., Dalton Trans*, 1987, 2359.

Paper 7/00964J; *Received* 11*th February*, 1997